Neutron Diffraction Study of KCN III and KCN IV at High Pressure*

D. L. Decker,† R. A. Beyerlein, G. Roult,†† and T. G. Worlton
Argonne National Laboratory, Argonne, Illinois 60439

The high pressure polymorphs of KCN, KCN III and KCN IV, have been investigated by neutron diffraction using a polycrystalline sample. Meaningful intensity measurements together with high resolution measurements of diffraction line positions confirm the structural description of KCN III but contradict the description of KCN IV suggested by previous high pressure x-ray work. The following picture emerges from our investigation. At a pressure of 25 kbar and at room temperature, KCN IV has a monoclinic structure with the C_s^3 space group in which the C and N nuclei are nearly along the body diagonal of a slightly distorted cube of K^+ ions. The conclusion from the x-ray work that KCN IV is rhombohedral is contradicted both by our intensity information and by the fact that several of the diffraction lines are displaced slightly from their exact rhombohedral positions. Increase of the temperature from 66°C to 74°C at a pressure of 22 kbar results in the transformation from phase IV into the cubic phase KCN III with the space group Pm3m (O_h^1) in which the CN^- molecules are ordered randomly along the eight equivalent [111] directions. The temperature factors in KCN III are unusually large indicating a high probability of a CN^- ion

---

*Based on work performed under the auspices of the U. S. Atomic Energy Commission.

†Present address: Dept. of Physics and Astronomy, Brigham Young University, Provo, Utah 84602

††Present address: Centre d'Etudes Nucleaires de Grenoble, Avenue Des Martyrs-38-Grenoble, France.

jumping between equilibrium positions along the eight diagonal configurations.

I. INTRODUCTION

The pressure-temperature phase diagram of KCN has been reported [1-3] and is shown over a restricted P-T range in Fig. 1. Recent neutron diffraction measurements[4] confirm that the I-V phase line shown by Pistorius et. al.[2] is in error as suggested in the note added in proof in that paper and thus it is not shown here. The structure of the high pressure phases of KCN have been examined via x-ray powder techniques[5,6] in an opposed anvil type apparatus. It is these phases, KCN III and KCN IV, with which we will be concerned in this paper. Richter and Pistorius[5,6] report KCN III as cubic, probably space group Pm3m (O_h^1) but their intensity data could not be used to help confirm this space group assignment. They made this assignment by analogy arguments from measurements on CsCN and TlCN. They also suggested that KCN III is disordered in that the CN^- ions either undergo a hindered rotation within the cubes of K^+ ions or that they randomly assume one of the 8 configurations along the 4 body diagonals. This latter structure could lead to a configuration entropy of R ln 8. Neutron diffraction measurements[4,7] in KCN I strongly suggest that the rotation model is incorrect. Pistorius[5] reported the KCN IV structure to be rhombohedral with the space group $R\bar{3}m$ (D_{3d}^5). He suggested that the linear CN^- ions are oriented but not ordered along the body diagonal. Again the intensities of the x-ray lines could not

be used to help determine the space group. The space group assignment was given using arguments from measurements on CsCN and a possible orientation entropy of R ln 2.[8]

Meaningful diffraction intensity measurements are possible with the high-pressure neutron diffraction apparatus[9] now at the CP-5 facility at Argonne. Such measurements could clarify many of the uncertainties in the understanding of these high pressure phases of KCN which were not cleared up by the x-ray studies. Thus we felt it of interest to measure the diffraction patterns of KCN III and KCN IV.[10] Our measurements confirm the structural description of KCN III but contradict the description of KCN IV suggested by previous high pressure x-ray work. KCN III is cubic with the space group Pm3m (O_h^1), while KCN IV is monoclinic with the space group Cm (C_s^3) rather than rhombohedral.

Measurements at different pressures and temperatures in phase IV yield a value of $\alpha = (.22 \pm .06) \times 10^{-3} {}^oC^{-1}$ for the volume thermal expansion and $\kappa = (1.43 \pm .33) \times 10^{-3}$ kbar^{-1} for the isothermal volume compressibility in this phase. The volume change between KCN III and KCN IV is $.38 \pm .07$ cm^3/mole at 22 kbar. This may be compared to Bridgman's value[1] of 0,22 cm^3/mole at 23 kbars from a piston-displacement measurement and Richter and Pistorius' value[6] of 0.49 cm^3/mole at 30 kbars from high pressure x-ray diffraction work. From our measurement and the slope of the III-IV phase line (.21 kbar deg^{-1}),[2] the entropy change between these two phases is calculated as R ln 2.62.

Although the measurement at 22 kbars and 66^{o}C appears to fall in the region previously reported as KCN III[2] we found that the KCN IV → III transition had not begun at this temperature and pressure, indicating a slight error in the previous determination

of the III-IV phase line.[2]

II. EXPERIMENTAL

A high purity KCN single crystal which was obtained from Susman and Hinks[11] was crushed with a mortar and pestle and loaded into a die inside a glove box, then pressed into pellets of 0.63 cm diameter. The pressure apparatus, a double acting piston-in-cylinder, has been described previously.[9,12] The only new feature was the method of heating the pressure chamber and sample and the temperature control. This was accomplished by heating a large bath of water and pumping the water through channels in an aluminum jacket around the binding ring. A thermocouple placed against the Al_2O_3 pressure chamber monitored the temperature and was used in a feedback circuit to control an auxiliary heater that kept the thermocouple reading constant to within $\pm$ 2°C.

The pressure at the sample was determined from a calibration of the pressure cell. This was accomplished by making several diffraction measurements of either pure NaCl in the sample chamber or mixtures of materials containing NaCl. The pressure was determined from the NaCl lattice spacing using Decker's equation of state.[13] In all cases the pressure versus load was repeatable to within $\pm$ 0.5 kbar to 30 kbar.

The neutron beam time of flight techniques have also been described.[12,14] The time of flight spectrometer was calibrated by taking diffraction patterns of Si and Ge[15] in the same position as the KCN sample. Diffraction spectra of KCN were taken at

the P-T points indicated in Fig. 1. The collection time for the KCN measurements ranged from 28 to 88 hours.

The phase changes in our pressure system were clean and sharp with complete disappearance of phase I at 25 kbar and room temperature and complete disappearance of phase IV at 74°C and 22 kbar. The disappearance of phase IV had not begun at 66°C and 22 kbar. These are indications of a good quasi-hydrostatic environment which is necessary in order to get meaningful intensity data from a powder sample for which one requires there be no preferential orientation of the crystallites.

III. RESULTS AND ANALYSES OF THE DIFFRACTION PATTERNS

Time-of-flight (TOF) neutron diffraction patterns with scattering angles of 60° are compared in Fig. 2 and Fig. 3 for KCN III and KCN IV. The data were initially analyzed by fitting the peaks individually by a least squares analysis to determine peak position and intensity. Tables I and II show that the positions of the diffraction peaks observed for KCN III are accurately indexed in a simple cubic lattice while some of the peak positions for KCN IV are displaced slightly from their exact rhombohedral values. This indicates that the actual structure of KCN IV is distorted from the rhombohedral.

To further analyze the TOF data we wrote a computer program that would simultaneously fit all the peaks with a Maxwellian background plus a time independent background using a least squares technique. The function of the count rate y_i in the i^{th} time channel is

$$y_i = b + M(\lambda_i) + \sum_{\vec{h}} \alpha_{\vec{h}} \exp\left[(-4\ell n2)(d_i - d_{\vec{h}})^2/S_i^2\right] + v \sum_{\vec{h}'} f_{\vec{h}'} \exp\left[(-4\ell n2\ (d_i - d_{\vec{h}'})^2/S_i^2\right] \quad (1)$$

where b is the time independent background, λ_i is the neutron wavelength scattered into channel i, $M(\lambda_i) = \beta d_i^{-\gamma} e^{-\delta/\lambda_i^2}$ is a Maxwellian intensity function with three variable parameters β, γ, δ used to fit the time-dependent background, d_i is the wavelength scattered into channel i divided by the factor $2\sin\theta$ where 2θ is the scattering angle (30 or 60 deg), and S_i is the instrumental linewidth at half peak height for each channel. The symbols $\vec{h}$ and $\vec{h}'$ stand for the Miller indices (hkℓ) for the KCN peaks and for the Al_2O_3 peaks respectively which might be present in the pattern. The calculated plane spacings for KCN and Al_2O_3, $d_{\vec{h}}$ and $d_{\vec{h}'}$, respectively, are determined from the lattice parameters which are the only adjustable parameters which affect the peak positions. $\alpha_{\vec{h}}$ and $f_{\vec{h}'}$ are the peak amplitudes of the KCN peaks and the Al_2O_3 peaks respectively, and v is an overall intensity factor for Al_2O_3. The KCN peak amplitudes $\alpha_{\vec{h}}$ are treated as variable parameters while the relative amplitudes $f_{\vec{h}'}$ for Al_2O_3 are held fixed at values determined from a pure Al_2O_3 diffraction pattern. Pb peaks, if present, are treated in the same manner as Al_2O_3 peaks. This allows an accurate subtraction of Al_2O_3 and Pb peaks from the pattern which in all cases were very small at the 60^o scattering angle. In some regions of the diffraction pattern the intensities obtained from

this type of analysis are slightly in error because the assumed shape for the Maxwellian, $\alpha\ d^{-\gamma}e^{-\delta/d^2}$, with the 3 variable parameters α, γ, and δ, is not sufficient to exactly fit the background over the entire spectrum. For the least squares technique here described the ratio of χ^2 to the number of degrees of freedom which we shall designate the "goodness of fit" should lie between 0.8 and 1.2 for a perfect statistical fit.

Since the TOF diffraction method employs a continuous range of neutron wavelengths (λ), the measured intensities are modified by the thermal neutron spectrum and by a λ^4 multiplication.[16]

Relative structure factors were determined from the measured intensities ($I_{\vec{h}}^{TOF}=\alpha_{\vec{h}}\ S_i(\pi/4\ell n2)^{\frac{1}{2}}$) according to the relation

$$m_{\vec{h}}|F_{\vec{h}}|^2 \propto \frac{I_h^{TOF}}{\lambda^4 I_o(\lambda)} \qquad (2)$$

where $m_{\vec{h}}$ is the multiplicity for the peak with label $\vec{h}$ in the diffraction pattern, $F_{\vec{h}}$ is the structure amplitude including Debye-Waller factors, and $I_o(\lambda)$ characterizes the neutron flux from the reactor. In our case $I_o(\lambda)$ was determined from a measurement of the direct beam transmitted through the pressure cell containing the sample using a detector matched to those used in the 30 and 60^o scattering angles, and so $I_o(\lambda)$ should implicitly contain absorption and multiple scattering corrections for both the sample and pressure cell as well as detector efficiency corrections. In fits to the diffraction pattern for well known cubic materials it was found that the measured $I_o(\lambda)$ predicted

structure factors for the diffraction peaks associated with the longer neutron wavelengths which were too low. In order to fit the measured intensities for well known cubic materials, the measured $I_o(\lambda)$ was adjusted for the longer neutron wavelengths by dividing it by $\sqrt{1 + (\lambda - 1.8)}$ for $\lambda > 1.8$ Å and by unity for $\lambda \leq 1.8$ before using it in Eq. (1) to calculate relative structure factors. We are not sure why this empirical correction is necessary, but different detector efficiencies could account for it.

In further analyzing KCN IV, we modified the least squares fitting technique summarized in Eq. (2) in order to test particular space groups. In this case the term $\alpha_{\vec{h}}$ for the amplitude of the KCN peak with label $\vec{h}$ in Eq. (1) is replaced by

$$\alpha_{\vec{h}} \rightarrow \frac{u\lambda_i^4 I_o(\lambda_i)}{S_i} \quad m_{\vec{h}} \; |F_{\vec{h}}|^2 \tag{3}$$

where u is an overall intensity scaling factor for KCN. This analysis was particularly useful in refining the KCN IV structure since the KCN IV diffraction pattern contained overlapping peaks.

Since our intensity measurements are important to our interpretation of the diffraction patterns for KCN III and IV we present in Table III our intensity results for KCN I at room temperature and compare them with the powder diffraction results in the literature.[7,17,18] Our measurements on KCN I were taken with the sample inside the pressure cell before application of

pressure. We have scaled our results so that the TOF value for the intensity ($|F|^2$) of the (200) diffraction peak agrees with the literature value.[7,17,18] Agreement is good except that the TOF value for the largest d-value peak (111) is slightly low. The good agreement with intensities obtained in previous powder neutron diffraction studies confirms the accuracy of our spectrum determination and the validity of the empirical correction discussed earlier.

For the KCN III pattern (Fig. 2) the diffraction peaks were well resolved and the peaks could be analyzed separately using Eq. (1) to determine the best value for the intensity of each peak. For the (110) diffraction peak there appear to be some small intensity "wings" above the background which may be due to thermal diffuse scattering, but no explicit allowance was made for this in the intensity analysis. The relative structure factors $|F_h^+|^2$ computed according to Eq. (2) were analyzed with a refinement program[19] to determine the position of the CN^- ion in the unit cell and the Debye-Waller factors for the K^+ and CN^- ions. Scattering lengths of $b_K = .37$, $b_C = .665$ and $b_N = .94$ in units of 10^{-12} cm per atom were assumed for the respective nuclei.[20]

Two different models were tried in the effort to determine the nature of the disordering of the linear CN^- molecules within the cubes formed by the K^+ ions in KCN III. Following Richter and Pistorius[6] we first tried the space group Pm3m (O_h^1) in which the K^+ ions were placed at the origin and the C and the N atoms were averaged over the eight equivalent (g) positions at x_1, x_1, x_1 along the [111] directions in the cubic unit cell. The eight CN scattering centers were each assigned a scattering length of $(b_C + b_N)/8$.

The midpoint of the CN bond was fixed at (1/2,1/2,1/2). In the refinement calculation[19] the thermal factors B_K, B_{CN} are given by the expression $e^{-B(h^2+k^2+\ell^2)/4a^2}$ prior to squaring in the structure factor where a is the lattice parameter for KCN III. The results of the refinement fitting are given in Table I. The position of the CN group resulting from the refinement was $x_1 = 0.407$ yielding a C-N bond length of $1.23 \pm .02$ Å along one of the 111 directions. The thermal factors $B_K = 2.6$ Å^2, $B_{CN} = 3.9$ Å^2 are large, reflecting the large amount of molecular libration present in this disordered system. Using the relation

$$B_{K,CN} = 8\pi^2 \langle \mu_x^2 \rangle_{K,CN} \qquad (4)$$

the linear motional amplitude $\langle \mu_x^2 \rangle^{\frac{1}{2}}$ is 0.18 Å and 0.23 Å for the K^+ and CN^- ions, respectively. The R value for the first ten peaks, of which only seven are clearly visible above the background was 4.1%. The large thermal factors reduced the amplitude of the peaks associated with the smaller lattice spacings below the statistical fluctuation in the background.

Next we tried a "free rotation" model[17] in which the K^+ ions were again fixed at the origin and the CN group was treated as a single entity which moved freely on the surface of a sphere whose center was at (1/2,1/2,1/2) and whose radius was one half the CN bond length. The best fit resulted for bond lengths in the range $1.20 \sim 1.24$ Å. The results for the fit with a bond length of 1.2 Å are tabulated in Table I. The R value for

this fit was R =11.5% which is to be compared with R = 4.1% for the fit to Pm3m (0_h^1). The "free rotation" model appears to be a poor model for KCN III.

IV. ANALYSIS OF THE KCN IV PATTERN

The rhombohedral analysis of the KCN IV data exposed two serious problems. First, several of the diffraction peaks were broadened in excess of the instrumental broadening and their shape was not truly gaussian, so that the fitting program summarized in Eq. (1) could not yield the correct intensities. Second, the (100), (200) and (210) diffraction peaks were displaced from their rhombohedral positions by more than the experimental uncertainty (Table II). The observed diffraction peak positions for KCN IV given in Table II are very nearly consistent with a rhombohedral lattice with unit cell constants $a_{rh} = 3.7803$ Å, $\alpha_{rh} = 86^{\circ}42'$.

On the basis of high pressure x-ray measurements, Pistorius[5] concluded that the most likely space group for KCN IV was $R\bar{3}m(D_{3d}^5)$. Here the K^+ ion is at (0, 0, 0) and the cyanide ion lies along the rhombohedral axis but without distinction between the heads and tails of the CN^-'s. Using the modification of our fitting program summarized in Eq. (3) we tested this model. The CN^- group was treated as a single entity with a scattering length $b_{CN} = (b_C + b_N)/2$. This "CN atom" was placed at (0, 0, z) and (0, 0, $\bar{z}$) in the hexagonal cell for which the c axis coincides with the primary axis of the rhombohedral cell. The K^+ ion was placed at the origin as before. The expression for the structure amplitude in Eq. (3) becomes

$$F_{\vec{h}} = \left[b_K \, e^{-B_K/4d_{\vec{h}}^2} + b_{CN} \, e^{-B_{CN}/4d_{\vec{h}}^2} \times 2\cos 2\pi \ell z \right] \times \left[1 + 2\cos(2\pi/3(-h + k + \ell)) \right] \quad (5)$$

This expression accounts for the equivalent origins in the hexagonal cell at (000), (1/3, 2/3, 2/3), (2/3, 1/3, 1/3). The fitting yielded a value for z = 0.4041, implying a CN bond length of 1.33 Å. The results for the temperature factors for the K^+ ions and the CN group were respectively, B_K = 1.67 $Å^2$ B_{CN} = 5.00 $Å^2$. The solid line in Figure 3 represents the best fit of the KCN IV diffraction pattern to $R\bar{3}m(D_{3d}^5)$. The poor intensity agreement apparent from the figure is reflected in the rather large goodness of fit value, 8.93 (See Section III). The displacement of the (100) and (200) diffraction peaks from their exact rhombohedral positions (Table II) is evident from Fig. 3. The apparent line broadening for several of the diffraction peaks ((100), (110) and (200)) which was apparent in the fitting summarized by Eq. (1) (no constraints on intensities) is also evident in Figure 3.

The diffraction peak broadening discussed above could arise either from a domain size effect[21] based on a short-range ordering of the CN^- molecule or from a distortion of the rhombohedral lattice to lower symmetry. The displacement of the (100) and (200) peaks from their positions in the rhombohedral lattice supplies a strong argument for the latter explanation.

Since the general indexing and intensities match those of $R\bar{3}m$ (D^5_{3d}) (Fig. 3) fairly well, the distortion from the rhombohedral structure must be small. Since the best values for the rhombohedral unit cell constants indicate only a slight distortion from the cubic KCN III structure, let us start from a model of KCN III sketched in Fig. 4. The space group $R\bar{3}m(D^5_{3d})$ with the cyanide ions lying along the rhombohedral axis (Fig. 3) is close to the real structure, so we start with the C and the N atoms lying along a three fold [111] axis in the cubic cell. If $\vec{a}_1$, $\vec{a}_2$, $\vec{a}_3$ ($|\vec{a}_1| = 3.808$ Å) are the edges of the cube we can describe this structure with an orthorhombic cell with

$$\begin{aligned} \vec{A}_1 &= \vec{a}_1 + \vec{a}_2 \\ \vec{A}_2 &= \vec{a}_1 - \vec{a}_2 \\ \vec{A}_3 &= \vec{a}_3 \end{aligned} \qquad (6)$$

We now have a C centered orthorhombic structure with two molecules per cell and CN^- lying in the (010) plane. We get the $R\bar{3}m(D^5_{3d})$ space group by increasing the length of the cube diagonal so that the angle α is smaller than 90° ($\alpha = 86^\circ 42'$). A small change in a is required to agree with the rhombohedral lattice parameter, a = 3.7803 Å, given above. The C-centered orthorhombic cell becomes a C centered monoclinic cell whose basis vectors $\vec{A}_1$, $\vec{A}_2$, $\vec{A}_3$, are also given by Eq. (6) if $\vec{a}_1$, $\vec{a}_2$, and $\vec{a}_3$ in

the r.h.s. of Eq. (6) are now taken to be the basis vectors for the rhombohedral cell.

There are three centered monoclinic space groups $C2(C_2^3)$, $C2/m(C_{2h}^3)$, and $Cm(C_s^3)$ which are subgroups of $R\bar{3}m(D_{3d}^5)$. $C2(C_2^3)$ and $C2/m(C_{2h}^3)$ give completely wrong intensities for all allowable positions of C and N and so we used the space group $Cm(C_s^3)$ with the C and N nuclei in the A_1A_3 plane of Fig. 4 which includes the primary rhombohedral axis of the undistorted cell. The nature of the monoclinic distortion from the rhombohedral can be inferred from the fact that the maximum "peak broadening" in the fit to the rhombohedral structure was observed for diffraction from planes normal to the principal diagonal of the rhombohedral structure. This implies a distortion of $\vec{A}_1$ and $\vec{A}_3$ but not of $\vec{A}_2$ in going to the monoclinic structure (Fig. 4). In what follows we describe the monoclinic cell with the parameters a, b, c, cosβ where, from Fig. 4,

$$\vec{A}_1 \rightarrow \vec{A}_1' \qquad A_1' = a$$

$$\vec{A}_2 \rightarrow \vec{A}_2' \qquad A_2' = b$$

$$\vec{A}_3 \rightarrow \vec{A}_3' \qquad A_3' = c \qquad \cos\beta = \frac{\vec{A}_1' \cdot \vec{A}_3'}{|\vec{A}_1' \cdot \vec{A}_3'|}$$

A fit of the KCN IV diffraction pattern to the space group $Cm(C_s^3)$ was done using the modification of our least squares fitting techniques described in Eq. (3) with the carbon nuclei at $(x_C, 0, z_C)$ and the nitrogen nuclei at $(x_N, 0, z_N)$. Symmetry requires that the C and N atoms lie in the plane pendicular to the unique

monoclinic b axis. This is a more general requirement than that indicated by their location along the primary rhombohedral axis of the undistorted cell shown in Fig. 4. The structure factor $|F_{\vec{h}}|^2$ in Eq. (4) becomes

$$|F_{\vec{h}}|^2 = A_{\vec{h}}^2 + B_{\vec{h}}^2$$

with

$$A_{\vec{h}} = b_K e^{-B_K/4d_i^2} + \left[b_C \cos 2\pi(hx_C+\ell z_C) + b_N \cos 2\pi(hx_N+\ell z_N)\right] e^{-B_{CN}/4d_i^2}$$

and

$$B_{\vec{h}} = \left[b_C \sin 2\pi(hx_C+\ell z_C) + b_N \sin 2\pi(hx_N+\ell z_N)\right] e^{-B_{CN}/4d_i^2} \qquad (7)$$

In the monoclinic cell $d_{\vec{h}}$ in Eq. (1) becomes[22]

$$d_{\vec{h}} = (1-\cos^2\beta)^{\frac{1}{2}} / \left[h^2/a^2 + k^2(1-\cos^2\beta)/b^2 + \ell^2/c^2 - 2h\ell\cos\beta/ac\right]^{\frac{1}{2}} \qquad (8)$$

All other parameters in Eq. (7) have been previously described. In the computer fit summarized in Eqs. (1), (4), and (7), the parameters a,b,c, $\cos\beta$, the lattice parameters for Al_2O_3, u, v, x_C, z_C, x_N, z_N, B_K, B_{CN}, α, γ, and δ were varied to yield a least square fitting to the data. This gives ten KCN crystal parameters using 53 peaks in the monoclinic structure. Most of these peaks are overlapping pairs or triplets but this analysis technique

can readily handle overlapping peaks. The results for the diffraction pattern taken at 25 kbar and 23°C are shown in Fig. 5 and Table IV. The monoclinic structure seems to account very well for the diffraction line positions. The fitting result for the monoclinic cell parameter, (Table IV) $\cos\beta = 0.0770 \pm .003$, rules out the possibility that the unit cell for KCN IV is orthorhombic. Some intensity discrepancies appear in the fit using the space group Cm (C_s^3). It is evident from Fig. 5 that the observed intensity for the (002) peak of the monoclinic pair (002), (220) is significantly lower than allowed in the best fit (solid line). The inset at the lower right of Fig. 5 showing a restricted region of the fit to the data for the 30° scattering angle shows the same discrepancy for the (001) peak of the monoclinic pair (001), (110). The experimentally observed intensity for the monoclinic pairs of diffraction lines labeled (401), (312) and (200), (111) in Fig. 5 is larger than allowed in the fit to Cm (C_s^3). The discrepancy for the (401), (312) and (200), (111) monoclinic pairs is far more serious in the fit to the diffraction pattern of KCN IV collected at 34 kbar and 23°C where it is also apparent that the observed intensity of the (400), (222) monoclinic pair is larger than allowed in the fit to C_s^3. These discrepancies might be due to the presence of preferred orientation which, according to the latter examples, becomes more pronounced with pressure. The application or reduction of pressure in a solid pressure medium can give rise to preferred orientation. Indeed, we found that, after release of pressure, the intensities observed for the (111) and (222) peaks in KCN I were reduced by a factor of two with respect to their values prior to the application of pressure (Table III) while the intensities for the other peaks remained unchanged.

The temperature factors for the K^+ and CN^- ions, B_K and B_{CN}, are smaller in KCN IV than in KCN III, indicating that the

ordering of the CN^- molecules is more complete in this phase. The value for B_{CN} in the fit to the diffraction pattern collected at 25 kbar, 23°C (B_{CN} = 2.80 Å^2, Table IV) gives a linear motional amplitude for the CN ion $\langle\mu_x^2\rangle_{CN}^{\frac{1}{2}}$ ∿ .19 Å (Eq. (4)) which is to be compared with the values B_{CN} = 4.0 Å^2, $\langle\mu_x^2\rangle_{CN}^{\frac{1}{2}}$ ∿ .24 Å for KCN III. The value for B_K in phase IV is essentially zero in contrast to the large B_K = 2.7 Å^2 found in phase III. (The result that the thermal factor for the potassium ion B_K has been reduced to zero in each of the above fits means that, in the course of the fitting, the statistical error for this parameter exceeded its value.) We suggest the following explanation for this result. In KCN I the large motional amplitude for the K^+ ions is associated with the local dilatations accompanying the rotational motions of the CN^- ion. This also seems a reasonable picture for KCN III. In KCN IV the ordering of the CN^- molecules is more complete, and it is likely that these rotational motions are largely absent. Consequently the local dilatations of the K^+ ions should be absent also.

Results for the computer fit to a third diffraction pattern for KCN IV (22 kbars, 66°C) are also summarized in Table IV. Comparison of the value for the C-N bond length 1.02 ± .06 Å with that obtained for the room temperature measurement at 25 kbars, 1.16 ± .03 Å, indicates that the C-N bond contracts somewhat as the temperature is increased in phase IV.

An attempt was made to fit the KCN IV data (25 kbars, 23°C) using the rhombohedral space group R3m (C_{3v}^5). This introduced an additional positional parameter in comparison with the fit to $R\bar{3}m(D_{3d}^5)$ since the C and N positions are now allowed to vary individually. However the fit was essentially different from that described for the space group $R\bar{3}m$ since the fitting program was modified to include the effect of preferential line broadening due to a domain size effect following

an analysis of domain line broadening for single crystal x-ray diffraction carried out by Evenson and Barnett.[21] Although the resultant fit reproduced the observed line shapes fairly well it could not account for the displacement of observed peak positions discussed above. This fit also could not account for the observed intensity for the diffraction line with rhombohedral indexing $(\bar{2}21)$. This discrepancy was pointed out for the monoclinic analysis since the monoclinic pair $(40\bar{1})$, $(31\bar{2})$ corresponds to the rhombohedral $(\bar{2}21)$ line in the undistorted cell. The goodness of fit ratio for this analysis (5.3) was significantly worse than the corresponding ratio for the monoclinic analysis (3.7).

V. DISCUSSION AND CONCLUSION

The KCN III phase seems to be understood reasonably well. The crystal structure is cubic with the space group $Pm3m(O_h^1)$. The diffraction peak intensities are well represented assuming a disordered crystal with the CN^- ion randomly distributed over the 8 diagonal configurations. The temperature factors are unusually large indicating a high probability of the CN^- ion jumping between equilibrium positions. The large motional amplitude for the K^+ ions may be caused by local dilatations accompanying the rotational motions of the CN^- ion. This dynamical picture is very similar to that proposed for KCN I.[4]

The KCN IV phase is more difficult to definitively interpret. There is some displacement of the $(\bar{1}00)$ and $(\bar{2}00)$ peaks from their exact rhombohedral positions ($\sim$ .014 Å and .007 Å, respectively) which, although small, is well outside the accuracy of the

experiment. This indicates some distortion of the rhombohedral structure. Such a distortion leads to a centered monoclinic lattice of space group Cm (C_s^3).

Two features of the monoclinic analysis of the KCN IV phase stand out. First the C and N atoms are ordered in the Cm(C_s^3) space group, allowing for the possibility that KCN IV is ferroelectric. There may be evidence for this in the fact that the (200), (111) monoclinic pair shows excess broadening over the instrumental line shape (Fig. 5). This may indicate some line broadening due to the presence of domains in the monoclinic structure. If this is so ferroelectric behavior would follow.

Second the temperature factors for the K^+ and CN^- ions, B_K and B_{CN}, are smaller in KCN IV than KCN III. The large temperature factors in KCN III are probably due in large part to the molecular libration which is present in this disordered system, so it is not surprising that the value for B_{CN} decreases upon passing to KCN IV where the CN molecules are partially ordered. It seems likely that the rotational motions of the rod-shaped CN molecules are largely absent in KCN IV. This would imply the absence of the local dilatations of the K^+ lattice present in a disordered system as KCN I.[4] This picture is consistent with our result that $B_K \approx 0$ in KCN IV.

Some intensity discrepancies remain. For the two orders of the (001), (110) monoclinic pair which were observed, the observed intensity for the (001) line is lower than allowed by the fit using the space group Cm(C_s^3). The observed intensity for the monoclinic

pairs (401), (312) and (200), (111) which are not fit well in the diffraction pattern collected at 25 kbar and 23°C (Fig. 5) are very poorly fit in the diffraction pattern collected at 34 kbars which also shows a similar discrepancy for the second order reflection of the (200), (111) pair. These discrepancies may indicate the presence of preferred orientation in KCN IV or may be due to an inadequacy in the assumed space group.

Results for measurements in phase IV at two different temperatures (Table IV) indicate that the C-N bond length contracts as the temperature is increased in phase IV although the value for bond length from the measurement at higher temperature ($1.02 \pm .06$ Å) is suspect due to the large uncertainty associated with it. Further increase of the temperature results in the transformation into the cubic phase III wherein the C-N bond length has lengthened to $1.23 \pm .02$ Å, a value which is slightly higher than the original value for the bond length $1.16 \pm .03$ Å in phase IV at room temperature. This result could be independently checked by infrared spectroscopy. It is also apparent from Table IV that the C and N nuclei are nearly along the body diagonal of a slightly distorted cube of K^+ ions in the C_s^3 structure. This is the case if $x_N = z_N$ and $x_C = z_C$ and even though the ratio of x/z in these analyses was completely free the best fit to that data is for them to be close to unity.

ACKNOWLEDGEMENTS

We wish to thank W. E. Evenson and J. D. Barnett for providing us with a copy of their domain broadening theory prior to publication and we wish to thank Sherman Susman for the KCN sample material. One of us (DLD) wishes to express thanks to the Office of Educational Affairs at Argonne for the fellowship which allowed him to work on this project at Argonne. One of us (GR) would like to express his appreciation to Argonne National Laboratory for the opportunity to stay at Argonne while this project was carried out.

Table I. Plane spacing and intensity of KCN III at 74°C and 22° kbar.

cubic hkℓ	d_{obs} (Å)	d_{calc} (Å)	$m\|F_{hk\ell}\|^2_{obs}$	$m\|F_{hk\ell}\|^2_{calc}$ Pm3m(O_h^1)	$m\|F_{hk\ell}\|^2_{calc}$ Free Rotation Model
100	3.807 ± .002	3.8080	16.38 ± 2.88	18.57	18.60
110	2.6912 ± .0011	2.6926	82.08 ± 5.64	79.79	79.00
111	2.1982 ± .0017	2.1985	5.84 ± 0.48	5.91	3.84
200	1.9049 ± .0007	1.9040	14.52 ± 1.74	14.49	16.09
210	*	1.7030	< 2.4	0.4	0.1
211	1.5538 ± .0016	1.5546	29.52 ± 2.64	30.87	27.02
220	*	1.3463	< 4.8	7.6	6.03
300 } 221	1.2694 ± .0028	1.2693	5.24 ± 3.32	5.51	6.45
310	*	1.2042	not observed	1.4	7.38
311	1.1498 ± .0016	1.1482	9.60 ± 2.40	9.68	8.82

Lattice Parameter = 3.8080 ± .0003 Å Unit Cell Volume = 55.22 + .01 $Å^3$	Refinement Fitting Parameters	
B_K ($Å^2$)	2.6	2.23
B_{CN} ($Å^2$)	3.9	6.21
C-N Bond Length (Å)	1.23	1.2
R Value for fit (%)	4.1	11.5

Table II. Calculated and measured positions for the spacings observed in KCN IV assuming a rhombohedral lattice. Only those peaks which could be resolved are listed.

hkℓ hex. indexing	Rhomb. indexing	d_{calc} (Å)	d_{obs} (Å)
101	100	3.7685	3.783 ± .002
012	110	2.7400	2.7405 ± .0011
110	$10\bar{1}$	2.5953	2.5954 ± .0004
003	111	2.3043	---
021	$11\bar{1}$	2.1375	2.1363 ± .0069
202	200	1.8842	1.8909 ± .0006
113	210	1.7231	1.7291 ± .0020
211	$20\bar{1}$	1.6500	1.6502 ± .0007
122	$21\bar{1}$	1.5248	1.5250 ± .0007
300	$2\bar{1}\bar{1}$	1.4984	1.4981 ± .0005
015	221	1.3215	1.3210 ± .0007
220	$20\bar{2}$	1.2976	1.2980 ± .0009

Lattice Parameters $a_{hex} = 5.1906 \pm .0003$ Å

$c_{hex} = 6.9129 \pm .0015$ Å

$a_{rh} = 3.7803$

$\alpha_{rh} = 86^{\circ}42'$

Volume of rhombohedral unit cell = $53.77 \pm .02$ Å^3

Table III. Comparison of time-of-flight intensity measurements on KCN I with previous powder diffraction results.

$hk\ell$	$\|F\|^2$(TOF)	$\|F\|^2$(Ref. 7)
111	1.8 ± .2	2.16
200	5.7 ± .5	5.72
220	3.7 ± .3	3.40
311	0.31 ± .06	0.25
222	1.9 ± .2	2.11

Table IV. Results of C_s^3 Analysis of KCN IV Phase.

P,T	25 kbars, 23°C	34 kbars, 23°C	22 kbars, 66°C
Goodness of fit	3.7	5.7	2.0
a	5.5303 ± .0013	5.5046 ± .0018	5.5166 ± .0024
b	5.2094 ± .0008	5.1885 ± .0011	5.2662 ± .0022
c	3.7429 ± .0009	3.7294 ± .0012	3.7579 ± .0020
cos β	0.0770 ± .0003	0.0826 ± .0004	0.0596 ± .0007
½ Unit Cell Vol. ($Å^3$)	53.76 ± .03	53.07 ± .05	54.49 ± .07
Carbon x,z	0.425 ± .004, 0.363 ± .004	0.433 ± .004, 0.371 ± .006	0.429 ± .006, 0.350 ± .008
Nitrogen x,z	0.587 ± .003, 0.542 ± .003	0.585 ± .003, 0.565 ± .004	0.570 ± .004, 0.514 ± .008
B_K ($Å^2$)	0.0	0.0	0.0
B_{CN} ($Å^2$)	2.80 ± .12	1.44 ± .12	4.56 ± .24
C-N bond length (Å)	1.16 ± .03	1.15 ± .04	1.02 ± .06

REFERENCES

1. P. W. Bridgman, Proc. Am. Acad. Arts Sci. 72, 45 (1937).
2. C. W. F. T. Pistorius, J. B. Clark, and E. Rapoport, J. Chem Phys. 48, 5123 (1968).
3. H. Suga, T. Matsuo, and S. Seki, Bull. Chem. Soc. Japan 38, 1115 (1965).
4. D. L. Price. J. M. Rowe, J. J. Rush, E. Prince, D. G. Hinks, and S. Susman, J. Chem. Phys. 56, 3697 (1972).
5. C. W. F. T. Pistorius, J. Phys. Chem. Solids 32, 2761 (1971).
6. P. W. Richter and C. W. F. T. Pistorius, Acta Cryst. B28, 3105 (1972).
7. M. Atoji, J. Chem. Phys. 54, 3514 (1971).
8. This is argued from an assumed R ln 8 configurational entropy in phase III and the change in entropy from slope and volume change along the III-IV boundary.
9. R. M. Brugger, R. B. Bennion, and T. G. Worlton, Phys. Lett. A24, 714 (1967).
10. G. Roult, R. Beyerlein, D. Decker, T. G. Worlton, Bull. of APS 18, 35 (1973).
11. D. G. Hinks, D. L. Price, J. M. Rowe and S. Susman, J. Crystal Growth 15, 227 (1972).
12. R. M. Brugger, R. B. Bennion, T. G. Worlton, W. R. Myers, Trans. Amer. Cryst. Ass. 5, 141 (1969).
13. D. L. Decker, J. Appl. Phys. 42, 3239 (1971).
14. D. L. Decker, and T. G. Worlton, J. Appl. Phys. 43, 4799 (1972).
15. The lattice parameters of Ge and Si were taken to be 5.65754^{o}A and 5.4307 A respectively.

16. B. Buras, Nukleonika 8, 259 (1963).

17. N. Elliott and J. Hastings, Acta. Cryst. 14, 1018 (1961).

18. A. Sequeira, Acta. Cryst. 18, 291 (1965).

19. W. R. Busing, K. O. Martin and H. A. Levy, "A Fortran Crystallographic Least Squares Refinement Program," Report ORNL-TM-305, Oak Ridge National Laboratory, Oak Ridge, Tennessee (1964).

20. G. E. Bacon, Acta. Cryst. A25, 391 (1969).

21. W. E. Evenson and J. D. Barnett, to be published.

22. "International Tables for X-ray Crystallography" (The Kynoch Press, Birmingham, England, 1965) Vol. I.

FIGURE CAPTIONS

Figure 1: Phase diagram of KCN for a restricted pressure-temperature range. The ⊗'s mark the P-T points corresponding to the measurements reported here. All other symbols are associated with phase boundary determinations as reported in Ref. 2.

Figure 2: Time-of-flight (TOF) neutron diffraction pattern for cubic KCN III. The solid line shows the result of simultaneously fitting all of the peaks letting the peak intensities be free. (See Section III of the text.) The fit is not extended to the (100) peak at the extreme right end of the pattern because of a frame overlap problem which caused the background to rise slightly here. The calculated position of the (100) peak is shown by a vertical arrow. The peaks due to the alumina (Al_2O_3) pressure cell are given with hexagonal indexing.

Figure 3: TOF neutron diffraction pattern for KCN IV. The solid line shows the result of simultaneously fitting all of the peaks assuming the space group $R\bar{3}m$ (D^5_{3d}) with the cyanide ion lying along the primary axis of the rhombohedral unit cell. (See Section III of the text.) The displacement of the (100) and the (200) peaks from their exact rhombohedral positions is emphasized by the inset above the (200) peak and the vertical arrow showing the calculated position of the (100) peak. The vertical lines just below the diffraction pattern give the rhombohedral line positions while the positions of the observable Al_2O_3 lines are marked by the symbol Y.

Figure 4: Relation of the crystallographic unit cells for KCN III and KCN IV. $\vec{a}_1$, $\vec{a}_2$, $\vec{a}_3$ are the edges of the cubic cell for KCN III and $\vec{A}_1$, $\vec{A}_2$, $\vec{A}_3$ are the edges of the C centered orthorhombic cell coinciding with the cubic cell. The monoclinic unit cell of KCN IV with edges $\vec{A}_1'$, $\vec{A}_2'$, $\vec{A}_3'$ slightly distorted from the orthorhombic vectors may be pictured as the result of a rhombohedral distortion followed by a monoclinic distortion along the [111] axis of the cubic cell. The C and N atoms, shown as lying along a [111] axis in the above figure, lie in ordered positions in the $A_1'A_3'$ plane in the monoclinic cell of KCN IV.

Figure 5: TOF neutron diffraction pattern for KCN IV. The solid line shows the result of fitting the observed diffraction pattern assuming that KCN IV is described by the centered monoclinic space group Cm (C_s^3) (See Section IV). The inset above and to the left of the (001), (1$\bar{1}$0) monoclinic pair shows the result of doing the above fit to the data for the 30° scattering angle. The vertical lines just below the diffraction pattern give the monoclinic line positions while the positions of the observable Al_2O_3 lines due to the pressure cell are marked by the symbol A.

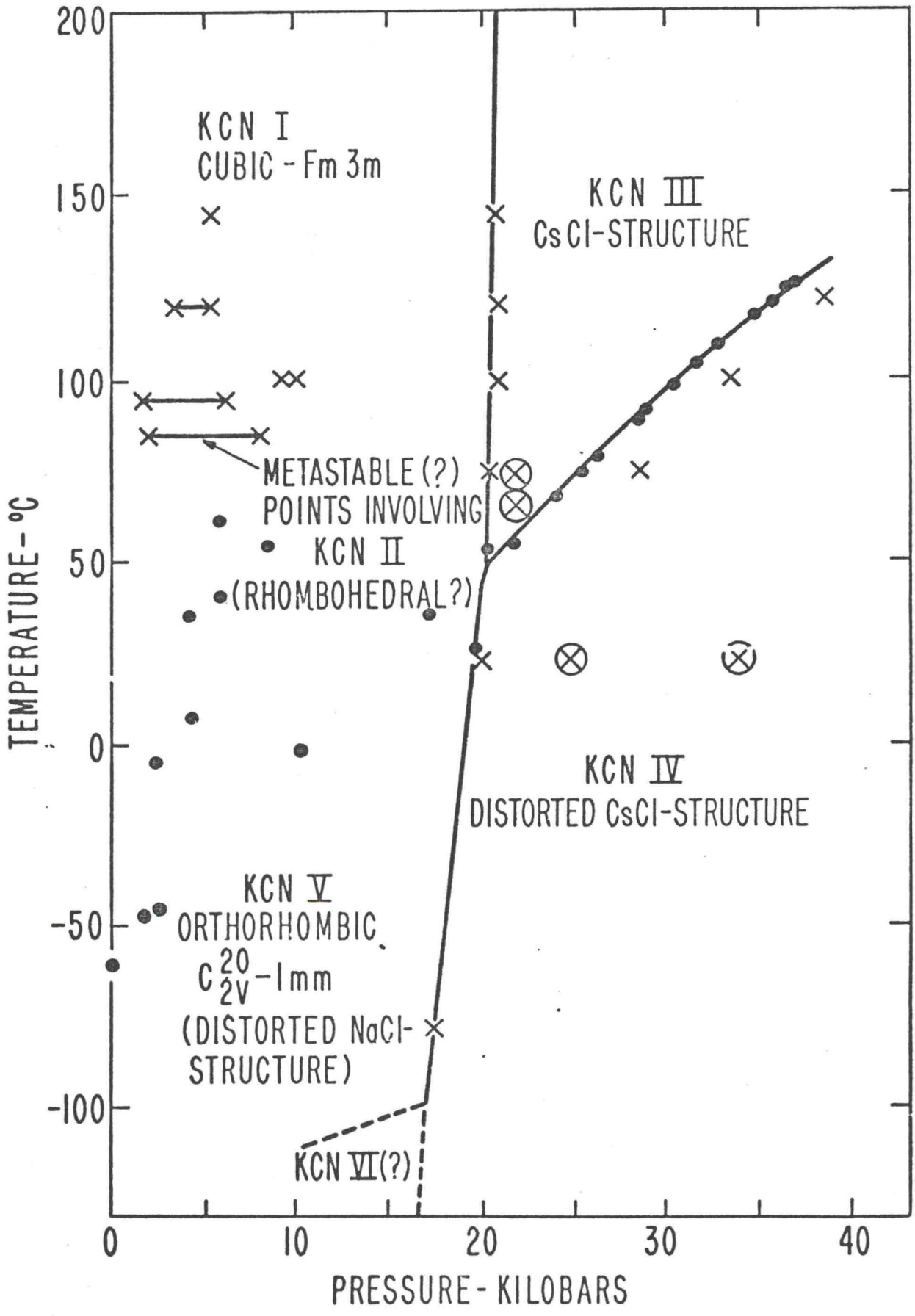
KCN I
CUBIC - Fm 3m
KCN III
CsCl-STRUCTURE
METASTABLE (?)
POINTS INVOLVING
KCN II
(RHOMBOHEDRAL?)
KCN IV
DISTORTED CsCl-STRUCTURE
KCN V
ORTHORHOMBIC
C_{2V}^{20} - Imm
(DISTORTED NaCl-
STRUCTURE)
KCN VI(?)
TEMPERATURE - °C
PRESSURE - KILOBARS
200
150
100
50
0
-50
-100
0
10
20
30
40

Figure 1

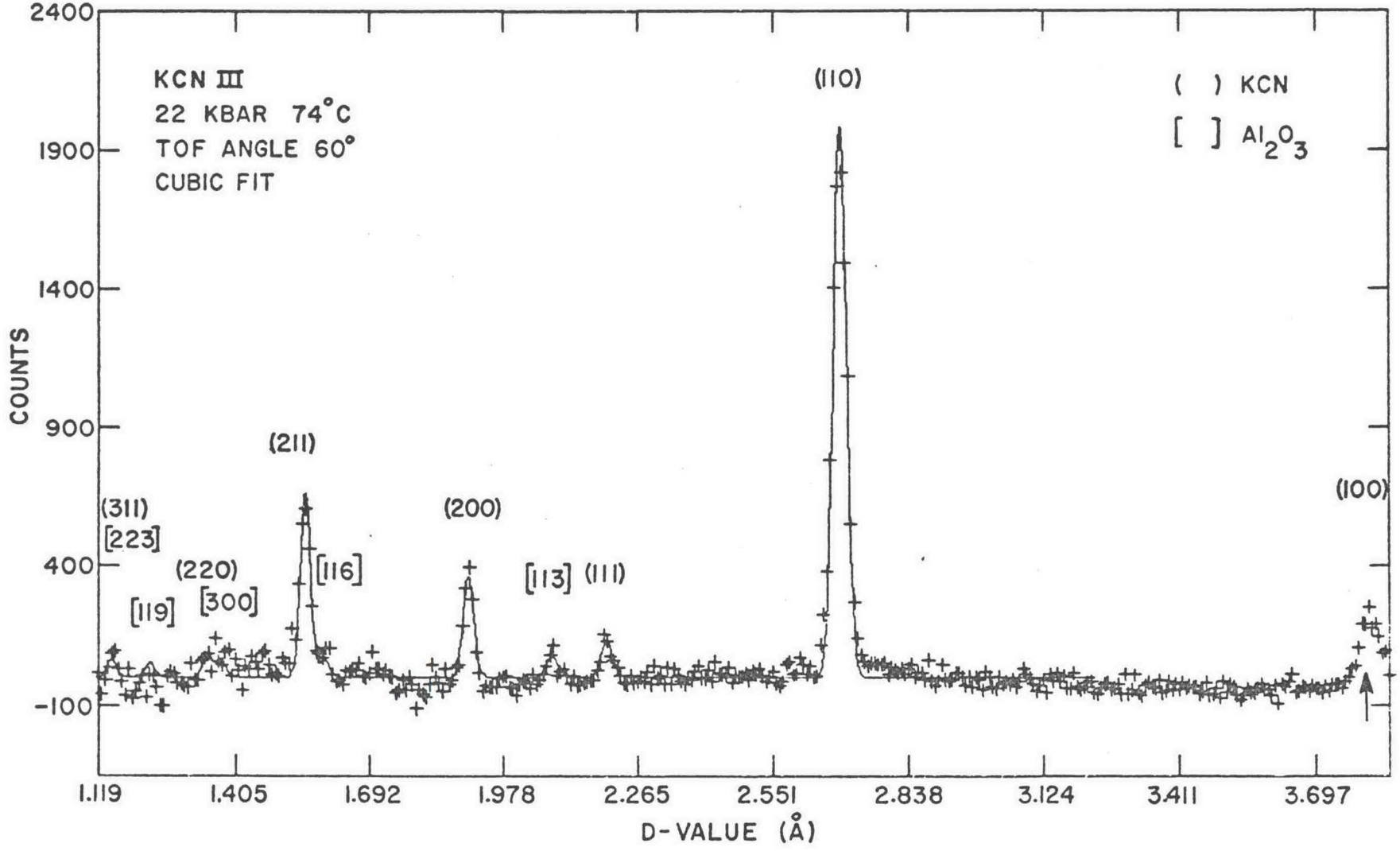
KCN III
22 KBAR 74°C
TOF ANGLE 60°
CUBIC FIT
( ) KCN
[ ] Al_2O_3
(110)
(211)
(200)
(100)
(311)
[223]
(220)
[300]
[119]
[116]
[113]
(111)
2400
1900
1400
900
400
-100
COUNTS
1.119
1.405
1.692
1.978
2.265
2.551
2.838
3.124
3.411
3.697
D-VALUE (Å)

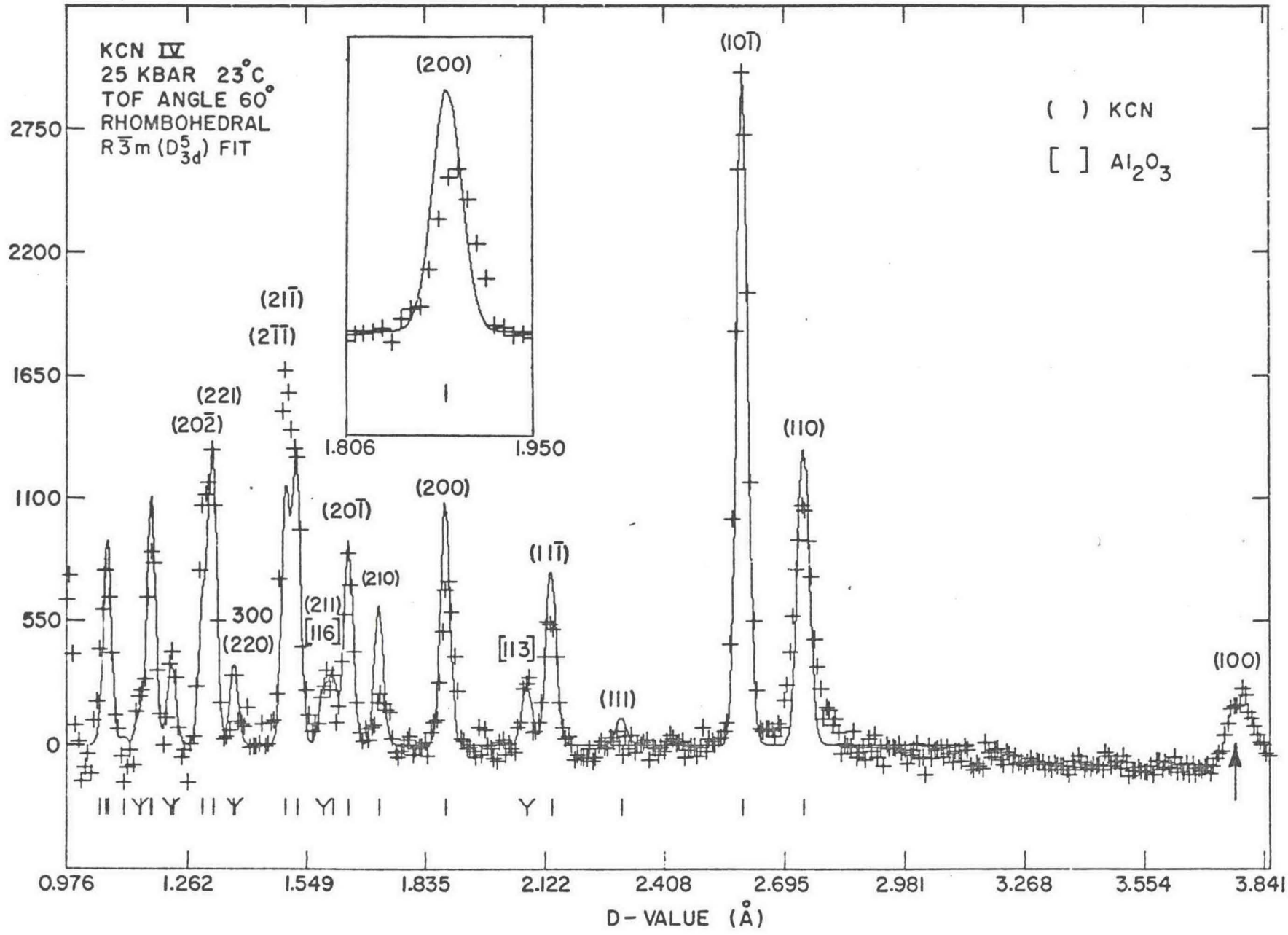
KCN IV
25 KBAR 23°C
TOF ANGLE 60°
RHOMBOHEDRAL
R$\bar{3}$m (D^5_{3d}) FIT
( ) KCN
[ ] Al_2O_3
(200)
1.806
1.950
(10$\bar{1}$)
(21$\bar{1}$)
(2$\bar{1}$1)
(221)
(20$\bar{2}$)
(110)
(20$\bar{1}$)
(200)
(11$\bar{1}$)
(210)
300
(220)
(211)
[116]
[113]
(111)
(100)
2750
2200
1650
1100
550
0
0.976
1.262
1.549
1.835
2.122
2.408
2.695
2.981
3.268
3.554
3.841
D-VALUE (Å)

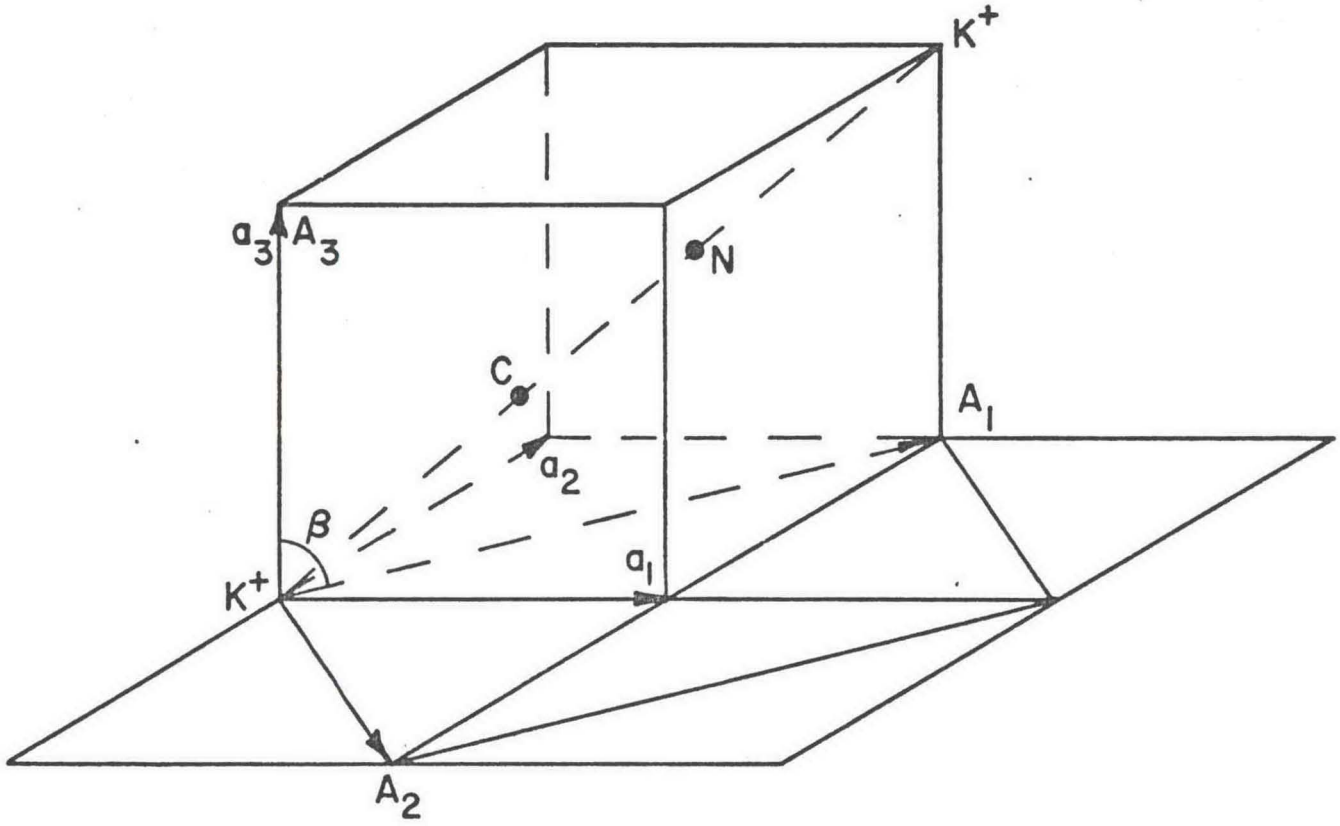
K+
a3
A3
N
C
A1
a2
β
K+
a1
A2

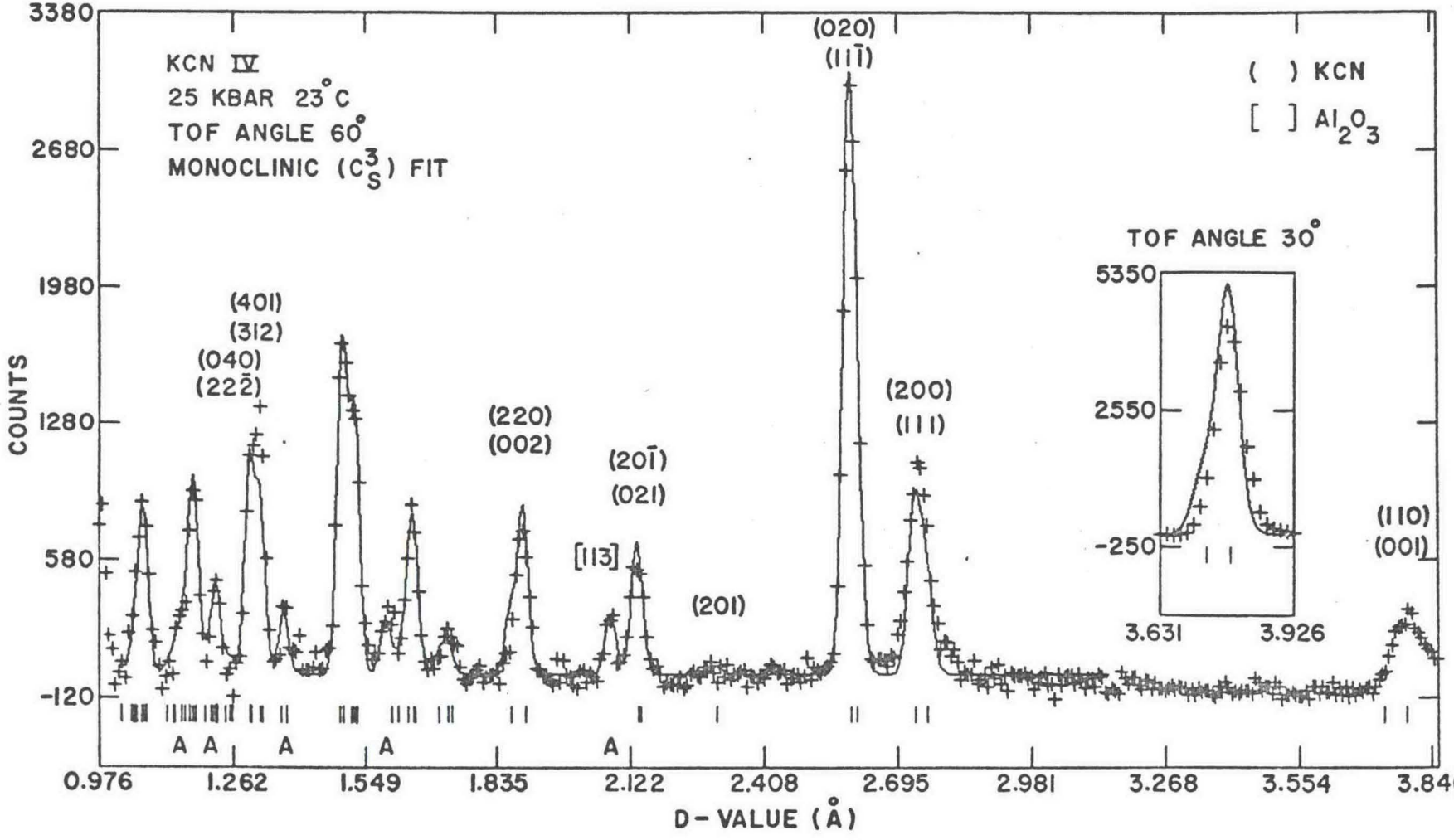
KCN IV
25 KBAR 23°C
TOF ANGLE 60°
MONOCLINIC (C_S^3) FIT
( ) KCN
[ ] Al_2O_3
TOF ANGLE 30°
COUNTS
D-VALUE (Å)
3380
2680
1980
1280
580
-120
5350
2550
-250
3.631
3.926
0.976
1.262
1.549
1.835
2.122
2.408
2.695
2.981
3.268
3.554
3.840
(020)
(11$\bar{1}$)
(200)
(111)
(110)
(001)
(401)
(312)
(040)
(22$\bar{2}$)
(220)
(002)
(20$\bar{1}$)
(021)
[113]
(201)
A A A A A

Figure 5